s-Tetrazine in Aqueous Solution: A Density Functional Study of Hydrogen Bonding and Electronic Excitations

Michael Odelius, Barbara Kirchner, and Jürg Hutter*

Physical Chemistry Institute, University of Zurich, Winterthurerstrasse 190, CH-8057 Zurich, Switzerland

Received: September 23, 2003; In Final Form: November 21, 2003

Using density functional theory based methods we studied vertical and adiabatic excitations of the s-tetrazine molecule, small clusters with water molecules and a single s-tetrazine molecule within 60 water molecules using periodic boundary conditions. We therefore achieve a consistent description of s-tetrazine from the isolated molecule to full solvation in water. The explicit treatment of solvent molecules allows for an accurate treatment of solute−solvent interactions. For the isolated s-tetrazine molecule a comparison with earlier high level ab initio calculations and other density functional calculations is made. In accordance with experiment the most favorable two−water-adduct displays a homodromic feature, i.e., a chain of hydrogen bonding from the nitrogen of the s-tetrazine to its methenyl (CH) group. Radial distribution functions calculated from a Car−Parrinello molecular dynamics simulation of the aqueous solution clearly show an unexpected preference of water for hydrogen bonding to the C−H group over the nitrogen lone pairs. Only infrequent and short-lived hydrogen bonds from water molecules to the nitrogen atoms are found. Calculations of vertical excitations using time-dependent density functional theory showed that the solvent shifts can be explained from the polarization of the Kohn−Sham orbitals of the solute. Hydrogen bonding has only a minor effect on the solvent shifts of low lying states of s-tetrazine.

1. Introduction

1,2,4,5- or s-Tetrazine (see Figure 1), the symmetric substituted azabenzene, has been a favorite with chemists for almost 100 years. The molecule, which forms water-soluble purple red crystals, has been extensively studied, and much effort has been devoted to characterize the ground and excited electronic states.

High-resolution spectroscopy[1] was used to investigate the $S_1 \leftarrow S_0$ transition in the visible region where several hundred strong peaks can be localized in four vibrational progressions. This absorption corresponds to a n $\rightarrow \pi^*$ transition. The geometry and vibrational spectra of both ground and first excited states are well characterized. However, other n $\rightarrow \pi^*$ transitions are mostly symmetry forbidden, and their locations are uncertain. $\pi \rightarrow \pi^*$ transitions similar to benzene were identified above 5 eV by energy electron-loss (EEL) and VUV spectroscopy.[2]

The wealth of well-resolved rotational and vibrational lines in the visible region have made s-tetrazine also a popular chromophore for the study of weakly bound systems in supersonic jets.[3,4] Complexes studied range from tetrazine bound to one or several rare gas atoms[5] to several polyatomic molecules. A specially interesting case is the s-tetrazine dimer,[6] where it was found that hydrogen bonding from one molecule to the π system or the lone pair of the other molecule was responsible for the binding. The possibility of hydrogen bonding was further investigated using clusters of s-tetrazine with HCl[7] and water.[8] These experiments led to detailed structures for the s-tetrazine−H_2O and s-tetrazine−2(H_2O) clusters.

The absorption spectra in water[9] shows a structureless peak at 510 nm, a shoulder at 305 nm and a further peak at 255 nm. The first two features are blue shifted with respect to spectra in cyclohexane and attributed to n $\rightarrow \pi^*$ transitions. The third peak does not show a shift from a cyclohexane solution and is assigned the first $\pi \rightarrow \pi^*$ transition. Whereas the origin of the first peak also in water has to be the strong n $\rightarrow \pi^*$ transition found in the gas phase, the assignment of the shoulder at 305 nm is uncertain. Typically, it is assigned either to a ^1A_u or $^1B_{2g}$ n $\rightarrow \pi^*$ transition in D_{2h} symmetry.

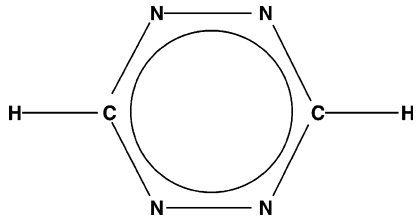

Figure 1. Lewis structure of s-tetrazine.

Important in these assignments are the interpretation of the peak as an adiabatic or vertical excitation since from theoretical calculations[10] it is expected that adiabatic values can be lowered by as much as one eV. Polarization measurements[11] on the emission as a function of the exciting wavelength support the assignment to a n $\rightarrow \pi^*$ transition.

The ^1A_u state was estimated by Innes[12] to lie at 3.4 eV. This estimate is based on an interpretation of the vibronic structure of the $S_1 \leftarrow S_0$ transition and a model for the interaction of the out-of-plane modes in the two excited states. The situation for s-tetrazine in aqueous solution can be summarized as follows. The first n $\rightarrow \pi^*$ transition shows a blue shift of 0.18 eV from the maximum of the peak in solution to the 0−0 transition in the gas phase and a blue shift of 0.09 eV to the maximum of the EEL spectrum. Further n $\rightarrow \pi^*$ transitions are estimated at 3.4 eV in the gas phase and seen as a shoulder in water at 4.06 eV. However, the uncertainty of the assignment and nature of these states prohibits the postulation of a solvent shift of 0.66 eV. A similar feature in the spectra measured in cyclohexane at 3.88 eV gives an estimate of a blue shift of 0.18 eV for this transition. Finally, the first $\pi \rightarrow \pi^*$ transition has a maximum

* Corresponding author. E-mail: hutter@pci.unizh.ch.

10.1021/jp0368381 CCC: $27.50
Published on Web 02/25/2004

in the EEL spectra at 5.0 eV and at 4.97 eV in VUV spectroscopy comparing to a maximum at 4.86 eV in water. Therefore, a red shift of 0.11−0.14 eV is estimated for this state.

The wealth of experimental data and the challenges from the assignment of states made s-tetrazine also an often studied molecule with quantum chemical methods. In an extensive study, Scheiner and Schaefer[10] used configuration interaction methods and coupled cluster methods to study vertical and adiabatic excitation energies, geometries and vibrational spectra in the ground and excited states, as well as possible mechanisms for photodissociation. Ågren et al.[13] used a multiconfiguration self-consistent reaction field theory to investigate solvatochromatic shifts in different azabenzenes. They found blue shifts for the first two $n \rightarrow \pi^*$ transitions and no effect on the first $\pi \rightarrow \pi^*$ transition in s-tetrazine. In a second-order perturbation theory investigation based on multiconfigurational wave functions (CASPT2) of the S_1 state using extended basis sets Schütz et al.[14] determined the vertical and adiabatic excitation energy. Later, Stanton and Gauss[15] used the equation-of-motion coupled cluster (EOMCC) method in a study of the S_1 $^1B_{3u}$ and the ^1A_u states. Most importantly, they found that the potential energy surfaces of the two states are connected through a lower symmetry path and they conclude that the ^1A_u state is a transition state and the indirect experimental evidence is related to a so-called cone state. In another coupled cluster investigation Del Bene et al.[16] addressed the problem again and concluded that under the assumption of an adiabatic excitation the assignment of the $^1B_{2g}$ state to the feature at 4.06 eV in the water spectrum is also possible. Further extensive studies of the vertical excitations of s-tetrazine up to 8 eV have been conducted using the CASPT2 method by Rubio and Roos[17] and the similarity transformed EOMCC method by Nooijen.[18] Time-dependent density functional theory (TDDFT) using the HCTH functional[19] was compared by Tozer et al.[20] to the CASPT2 results of Rubio and Roos.[17] Recently, Adamo and Barone[21] combined a polarizable continuum model[22] (PCM) with the density functionals PBE[23] and PBE0[24] to study solvatochromic shifts for the first excited states of s-tetrazine. They found improved excitation energies using hybrid functionals and concluded that a mixed cluster continuum model yields the best description of solvatochromic effects.

The goal of the present study is to investigate the influence of hydrogen bonding on the electronic states of s-tetrazine. Using density functional theory based methods we studied vertical and adiabatic excitations of the s-tetrazine molecule, small clusters with water molecules and a single s-tetrazine molecule within 60 water molecules using periodic boundary conditions. We therefore achieve a consistent description of s-tetrazine from the isolated molecule to full solvation in water. The explicit treatment of solvent molecules allows for an accurate treatment of solute−solvent interactions.

The paper is structured as follows. In the next section we describe the computational approaches used in detail. In section 3, results for the s-tetrazine molecule in the ground and excited states are given, and different computational and theoretical approaches compared. In section 4, we study the microsolvation of s-tetrazine with up to four water molecules. Car−Parrinello molecular dynamics simulations[25] combined with TDDFT calculations of the excitation spectra are presented in section 5. Finally, a summary and conclusions end the presentation.

2. Computational Methods

All-electron calculations with local basis sets were carried out with programs from the TURBOMOLE 5.6 package.[26] In these calculations we made use of Dunning's aug-cc-pVTZ correlation consistent basis set[27,28] and Ahlrichs' TZVP basis set, i.e., TZV kernel[29] plus polarization functions from Dunning's cc-pVTZ basis.[27] Excitation energies and forces in the excited states are calculated from linear response theory to TDDFT.[30] All frequency analyses were undertaken within the harmonic approximation by numerical first derivatives of analytical gradients of the total electronic energy applying the SNF program package.[31] The calculated interaction energies were obtained via the supermolecular approach. All values are counterpoise[32] corrected. The corrections were in all cases smaller than 1 kJ/mol per hydrogen bond.

Car−Parrinello molecular dynamics[25] calculations were performed using the CPMD program.[33,34] This program is based on a plane wave basis expansion of the valence electronic wave functions combined with a pseudopotential approach. We used norm-conserving pseudopotentials, expressed in the Kleinman−Bylander form,[35] with a 70 Ry kinetic energy cutoff for the plane wave expansion. For hydrogen a local pseudopotential parametrized with one Gaussian was used.[36] The pseudopotentials for carbon, nitrogen and oxygen were of Troullier-Martins type[37] and were nonlocal in the s angular momentum only. In the pseudopotential generation, the cutoff radii were set to 1.23 au(C), 1.12 au(N), and 1.05 au(O) for all angular momenta.

The aqueous solution of s-tetrazine was modeled by a single solute molecule in a solution of 60 water molecules in a cubic simulation cell with a box length of 12.4 Å and periodic boundary conditions. The CPMD simulation was initialized from a classical molecular dynamics simulation and was equilibrated for 3 ps at 300 K with a Nosé−Hoover thermostat[38,39] coupled to the ionic degrees of freedom. Subsequently, the system was simulated at 300 K for 2 ps. All hydrogens are deuterated and a 5.0 au time step in combination with a 700 au fictitious electron mass was used in the Car−Parrinello dynamics.[25] To understand the physical origin of solvent shifts in the electronic excitations, the results from the Car−Parrinello molecular dynamics simulations were compared to a mixed density functional/classical force field treatment (QM/MM) in which only the electronic degrees of freedom of the solute were included in the electronic structure calculations. Since, we are only interested in how the QM/MM description influences the electronic spectrum and not in effects on the solvent structure, the atomic coordinates are taken directly from the full DFT treatment. The solvent molecules were described by the flexible TIP3P[40] potential model from the AMBER94 force field.[41] The van der Waals interaction were derived using the atom types CQ/NC for the sp2 carbon/nitrogen in six membered rings in AMBER94.[41] The electrostatic interactions between the quantum system and the molecular mechanics system are treated according to Ref 42, in which in particular "charge spill-out" due to the classical point charges is avoided.

Excitation energies in the periodic systems are calculated within the Tamm−Dancoff approximation to TDDFT.[43,44]

All calculations in the ground state were performed using the BLYP[45,46] and B3LYP[47,48] density functionals. The same functionals were also used in TDDFT calculations. The Car−Parrinello simulations used the BLYP functional only.

3. Ground and Excited States of Isolated s-Tetrazine

There are several high level ab initio calculations[10,14−18,49] as well as other density functional calculations[20,21] available for the ground and excited states of s-tetrazine. This allows to check the reliability of the functionals and basis sets used in the present work. Both functionals, BLYP and B3LYP show the same order

TABLE 1: Vertical Excitations of s-Tetrazine As Obtained with Different Methods[a]

symmetry	character	BLYP	B3LYP	CASPT2[b]	EOMCC[c]	PBE[d]	PBE0[d]	expt
$1B_{3u}$ n → π^*	$3b_{3g} \rightarrow 1a_u$	1.88	2.21	1.96	2.22	1.78	2.23	2.25[e]
$1A_u$ n → π^*	$3b_{3g} \rightarrow 2b_{3u}$	2.86	3.38	3.06	3.62	2.68	3.45	3.4[f]
$1B_{1g}$ n → π^*	$5b_{1u} \rightarrow 1a_u$	4.12	4.71	4.51	4.73	4.10	4.86	
$1B_{2u}$ $\pi \rightarrow \pi^*$	$1b_{2g} \rightarrow 1a_u$	5.39	5.70	4.89	4.90	5.65	5.83	4.97[g]

[a] Values are in eV; for basis sets, see previous tables and ref 21. [b] Reference 17. [c] Reference 49. [d] Reference 21. [e] 0−0 transition.[9] [f] Estimated.[12] [g] Reference 2.

TABLE 2: Adiabatic Excitation Energies of the First Excited States of s-Tetrazine[a]

symmetry	transition	character	BLYP	B3LYP	expt
$1B_{3u}$	n → π^*	$3b_{3g} \rightarrow 1a_u$	1.75 (−0.13)	2.07 (−0.14)	2.25[b]
$1A_u$	n → π^*	$3b_{3g} \rightarrow 2b_{3u}$	1.93 (−0.93)	2.38 (−1.00)	3.4[c]
$1B_{1g}$	n → π^*	$5b_{1u} \rightarrow 1a_u$	4.10 (−0.02)	4.68 (−0.03)	

[a] Values in parentheses are shifts from the vertical excitation energies. All values in eV. [b] 0−0 transition.[9] [c] Estimated.[12]

TABLE 3: Optimized Geometries of s-Tetrazine in Several Excited States[a]

state	method	*r*(C−H)		*r*(C−N)		*r*(N−N)		∠(N−C−N)	
$1B_{3u}$	BLYP	108.7	−0.2	133.9	−0.7	133.2	−0.6	121.3	−5.4
	B3LYP	107.9	−0.3	132.7	−0.6	131.3	−0.5	120.8	−5.4
	CASPT2	107.3	−0.1	133.3	−0.5	132.1	−0.5	121.4	−5.1
	expt	106.3	−0.1	132.4	−1.7	134.9	2.3	123.2	−3.2
$1A_u$	BLYP	107.6	−1.3	139.2	4.6	124.0	−9.8	115.8	−10.9
	B3LYP	107.0	−1.2	138.0	4.7	122.4	−10.9	115.3	−10.9
	EOM-CC	107.9		139.0		124.0		115.9	
$1B_{1g}$	BLYP	109.0	0.1	134.8	0.2	126.4	−7.4	117.4	−9.3
	B3LYP	108.0	−0.2	133.6	0.3	124.8	−7.0	117.0	−9.2

[a] All optimizations were performed in D_{2h} symmetry (distances are in pm and angles in deg). After each parameter the difference to the ground state is given: CASPT2 values from ref 14; EOM-CC values from ref 15; experimental values from ref 1.

of Kohn−Sham states. However, as expected the hybrid functional B3LYP has the occupied orbitals shifted to lower energies and the virtual orbitals to higher energies. Symmetry labels (in D_{2h} symmetry) and character of the highest occupied and lowest unoccupied Kohn−Sham orbitals can be found together with the ground-state geometries and harmonic frequencies in the Supporting Information. Calculated ground-state geometries from density functional theory and from previous studies using CCSD(T) and CASPT2[14] are close to the experimental values, with maximal deviations of less than a degree for the N−C−N angle and 1.6 pm in the C−H bond length. Good agreement is also achieved for harmonic frequencies in the ground state when compared to the CCSD(T) calculations from reference[14] as well as to experiments (see Supporting Information). The DFT calculations support the observations of Schütz et al.[14] and Scheiner and Schaefer[10] regarding the splitting of the C−H stretch vibration. Namely, all theoretical calculations show a minimal splitting whereas in the experiment an 80 cm^{-1} difference between the symmetric and antisymmetric mode is reported. We find an overall better agreement of the results from the BLYP functional with coupled cluster calculations, than with the hybrid functional B3LYP. Recently, Rauhut and Werner[50] have found similar results in their study of vibrational spectra of furoxanes using different types of (hybrid −) functionals.

In Table 1 vertical excitation energies for the first three n → π^* and the first $\pi \rightarrow \pi^*$ transitions are listed. Similar trends can be observed for the pure density functionals BLYP and PBE. The n → π^* transition energies are underestimated, and the $\pi \rightarrow \pi^*$ transition energy is overestimated. Consistently, the BLYP functional gives results closer to experiment and the CASPT2 and EOM-CC calculations than PBE. Very similar results were also found by Tozer et al.[20] for the HCTH functional. The two hybrid functionals give results very close to each other and excitation energies for the n → π^* transitions are within 0.24 eV from the EOM-CC results. However, the $\pi \rightarrow \pi^*$ $1B_{2u}$ energy is overestimated by about 0.7 eV. These results are consistent with systematic studies of other aromatic molecules.[20,51] Tozer et al.[20] studied an extended set of transitions in s-tetrazine, including states of doubly excitation character and Rydberg-like states. They showed that density functionals of the type used in the present study perform very poorly for these transitions. Some of these states, e.g. the 2^1A_g state have a lower excitation energy than the first $\pi \rightarrow \pi^*$ state and are missing in the DFT treatment. For our study of solvation effects and comparison to available experimental data, however, these states are not of primary importance. Table 2 lists the adiabatic excitation energies for the three lowest n → π^* transitions. The change of excitation energies is almost identical for calculations with the BLYP and B3LYP functionals. A very small change for the B_{1g} state and a shift of about 0.13 eV is found for the first excited B_{3u} state. These values agree with earlier calculations,[10,14,15] and also the large shift (≈ one eV) for the A_u state is correctly reproduced by the density functional calculations.

Table 3 lists the geometries as obtained after optimization in the excited states and the differences to the ground state geometry is listed after each geometrical parameter. If the entry has a negative value, it indicates a contraction of the corresponding geometrical parameter in the excited states. The geometries optimized in the different excited states are affected differently. Only small changes are found in the geometry of the first excited state, all distances are contracted by approximately $^1/_2$ pm. All methods predict the N−C−N angle to become smaller on excitation. In accordance with the CASPT2 calculation the density functionals predict a slight contraction of the N−N bond length whereas the experimental value is 2.3 pm larger. For the $1A_u$ drastic changes in parameters are displayed in the case of the N−N bond and the N−C−N angle: They are contracted by up to 10 pm and 10 deg, respectively. This goes together with an elongation of the C−N

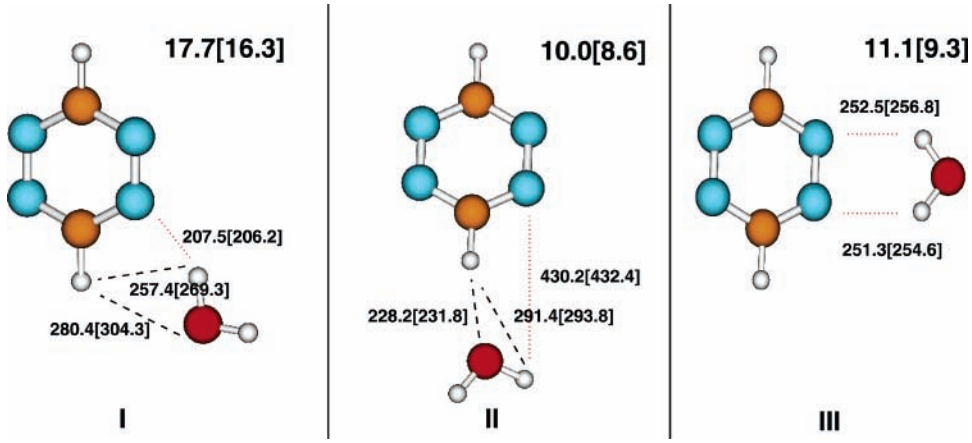

Figure 2. Different possible structures for s-tetrazine with one water molecule. Critical distances calculated using the B3LYP (BLYP values in parentheses) are marked (pm). Interaction energies in the right upper corner are given in kJ/mol.

distance and a slight shortening of the C−H bond. The N−N bond and the N−C−N angle are strongly contracted in the $1B_{1g}$ state whereas the other distances are only slightly changed. Results from the BLYP functional and those from B3LYP differ by at most 2 pm and 0.5 deg, despite the fact that rather large differences in excitation energies are present.

Harmonic frequency analysis of the optimized excited states structures revealed a large imaginary frequency for the D_{2h} symmetrical $1A_u$ state. The same behavior was already found by Stanton and Gauss[15] and they remarked that following this mode into the C_{2h} subspace of geometries leads to the D_{2h} structure of the S_1 state. The imaginary frequency found in their EOM-CC study using a DZP basis set was $1584i$ cm^{-1}, whereas our corresponding B3LYP value is $1365i$ cm^{-1} and the BLYP value is $1062i$ cm^{-1}.

In the investigation of the vibronic coupling between the S_1 state and a possible nearby $1A_u$ state, Innes[12] concluded that the energy gap between the two states, at the geometry of the S_1 state should be ≈9600 cm^{-1}. The corresponding value was calculated by Stanton and Gauss[15] to be 9840 cm^{-1}, and we find a value of 8471 cm^{-1} for the B3LYP functional.

4. Microsolvation: s-Tetrazine−Water Adducts

Adding one to four water molecules to s-tetrazine is used to study the patterns of hydrogen bonding under microsolvation conditions and its effect on the excited states. Experiments provide valuable tests for our calculations.

Original experiments on s-tetrazine dimers by Haynam et al.[6] could be explained assuming hydrogen bonding between the two molecules. Different shapes with either the hydrogen atom of one s-tetrazine interaction with a nitrogen lone pair or the π electron cloud of the other molecule were found. These experiments were followed by the same group using the strongly hydrogen bonding molecules HCl[7] and water.[8] In both cases it was found that the first molecule forms a hydrogen bond to the nitrogen of s-tetrazine and subsequently added molecules form water−water or HCl−HCl hydrogen bonds in a chain like alignment, see structure **IV** in Figure 3.

Figure 2 shows three structures for the dimer adduct which were optimized in order to get insight into hydrogen bonding. It also gives the interaction energies for each adduct together with some bond distances from the B3LYP calculations (BLYP in parentheses). In addition to the structures **I**−**III** in Figure 2 we also optimized structures with the water molecule interaction directly to the π-system of the s-tetrazine molecule. Surprisingly, the most stable configuration has a structure with one O−H bond parallel to the s-tetrazine ring and the other hydrogen pointing away from the π-system. The same structure was obtained using the MP2 method with a TZVP basis set. The interaction energy is 7 kJ/mol (5 kJ/mol), considerably lower than that for the other structures.

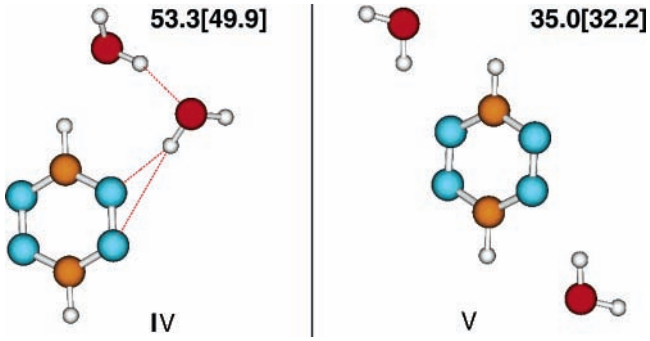

Figure 3. Adducts of s-tetrazine with two water molecules. Interaction energies are given in the right upper corner in kJ/mol for the B3LYP functional, with BLYP values in brackets. Hydrogen bonds for structure **IV** are given in Table 5.

The arrangement in structure **II** can be considered as a C−H···O hydrogen bond. This is reflected in the interaction energy of 10.0 kJ/mol. The arrangement in **III** gives an energy of 11.1 kJ/mol. The strongest interaction energy is found in structure **I** (17.7 kJ/mol). This energy is comparable to the interaction energy of the water dimer. However, in structure **I**, a donor and acceptor position of the water molecule are occupied and cannot be further used in a hydrogen bonding network. The binding energy should therefore be compared to that of two hydrogen bonds in water. A similar argument applies to structure **III**. This makes structure **II** the most compatible structure to be included into the water network. The hydrogen bonding of s-tetrazine in aqueous solution will be investigated using Car−Parrinello simulations shown in section 5.

In Table 4, the geometries of the s-tetrazine as adduct with one and two water molecules are listed. The deviations from the isolated s-tetrazine are listed next to each parameter. A negative sign indicates contraction, as in the case of the excited state geometries for the isolated s-tetrazine. Only the values for the bonds and bond angles on the bonding side are given.

Small changes to the geometry of the isolated s-tetrazine can be found. A reduction of the size of the N−C−N angle in all cases, in the **I** adduct, a contraction of the N−N bond and in the **II** adduct, and increased C−N distance are found. This is reasonable considering the fact that the **I** adduct has a hydrogen bond mainly to the nitrogens with some distortion to the

TABLE 4: Geometries of s-Tetrazine and Its Adduct with Water Molecules in the Ground State[a]

structure	method	r(C−H)		r(C−N)		r(N−N)		∠(N−C−N)	
				+ $1H_2O$					
I	BLYP	108.8	−0.1	134.6	−0.0	133.6	−0.2	126.1	−0.6
	B3LYP	108.2	0.0	133.3	0.0	131.6	−0.2	125.6	−0.6
II	BLYP	108.9	0.0	134.9	0.3	133.8	0.0	126.3	−0.4
	B3LYP	108.3	0.1	133.6	0.3	131.8	0.0	125.7	−0.5
III	BLYP	108.8	−0.1	134.5	−0.1	133.8	0.0	126.5	−0.2
	B3LYP	108.2	0.0	133.2	−0.1	131.8	0.0	125.9	−0.3
				+ $2H_2O$					
IV	BLYP	109.1	0.2	134.8	0.2	133.7	−0.1	125.4	−1.3
	B3LYP	108.4	0.2	133.5	0.2	131.7	−0.1	125.0	−1.2
V	BLYP	108.8	−0.1	134.7	0.1	133.5	−0.3	126.0	−0.7
	B3LYP	108.2	0.0	133.4	0.1	131.5	−0.3	125.5	−0.7

[a] Distances are in pm and angles in deg. After each parameter the difference to the isolated s-tetrazine is given.

hydrogen at the carbon, (see Figure 2) and that the **II** adduct forms a hydrogen bond from the oxygen of the water molecule to the C−H group of the s-tetrazine.

Water addition has only a small influence on the harmonic frequencies of the s-tetrazine molecule. For dimer **I** maximum deviations are less than 10 cm^{-1}. One finds red shifts for the "boat deformation" and for the "C−H in plane wag" and blue shifts for the "asymmetric C−H stretch" and the "symmetric C−H stretch". Comparing the spectrum from harmonic frequency analysis of the isolated s-tetrazine to the dimer **II**, which shows the 10 kJ/mol strong hydrogen bond to the C−H moiety, a blue shift can be found for all vibrations involving the C−H group. In the case of the "out-of-plane C−H wag" a blue shift of 30−40 cm^{-1} is seen, and for the C−N stretch the frequency is increased by 18 cm^{-1}, which is reflected in the elongation of this bond; see Table 4. Hydrogen bonding of the type found in structures **I** and **II** has recently been of considerable interest.[52] In particular, the blue-shifted C−H stretch frequencies were used as argument to propose a new type of hydrogen bond. However, it has been shown that the physical origin of this type of interaction is the same as in the stronger hydrogen bonds[53] and that the blue shift in the stretching frequency does not have to be accompanied by a shortening of the bond.

For the two−water adduct only two cases were considered (see Figure 3), structure **IV** displays again a homodromic character (a unstrained ring structure build of hydrogen bonds) and the second structure is build by adding each water molecule at different positions, similar to structure **I** of the dimers. Table 4 also gives the geometries of the two−water adducts. An elongation of the C−H bond can be observed for the trimer structure **IV**. This is probably due to the more relaxed situation of the chain of hydrogen bonds compared to the dimer adduct structure **I**. The formation of a hydrogen bond is in this case possible like in the case of structure **II** of the dimer adduct. We see again for the second structure **V**, a slight shortening of the C−H bond and a shortening of the N−N bond. Additionally the N−C−N angle gets smaller. The favorable arrangements of the geometry is reflected in the interaction energies. While the second structure gains two hydrogen bonds (17.7 [16.3] kJ/mol) of the type observed in dimer structure **I**, resulting in 35.0-[32.2] kJ/mol, the first structure cannot be explained by simple additivity. The total hydrogen bond energy would be in this case only 37.6 kJ/mol, whereas we find 53.3 [49.9] kJ/mol. This clearly shows that that hydrogen bonding favors structures where cooperative effects can play a role. The C−H···O contribution in trimer **IV** cannot be simply estimated as it shows a highly nonadditive behavior. In general, it can be observed that hydrogen bond energies increase by involving complicated "more than one-contact" situations.[54]

TABLE 5: Comparison of Experimental and Calculated Geometries of s-Tetrazine Adducts[a]

+ $1H_2O$ structure **I**				
method	$r(O_w-N_t)$	$r(H_w-N_t)$	$\angle N_tO_wH_w$	$\angle N_tN_tO_w$
expt	297	212	22	108.7
BLYP	295.8	206.2	19.8	126.8
B3LYP	292.0	207.5	24.2	121.1
+ $2H_2O$ structure **IV**				
method	$r(O_w-N_t)$	$r(H_w-N_t)$	$\angle N_tO_wH_w$	$\angle N_tN_tO_w$
expt	300	210	8.1	143
BLYP	293.1	197.5	11.9	140.2
B3LYP	292.2	197.9	12.2	140.1

[a] Distances are in pm and angles in deg.

In Table 5, we compare the hydrogen bonds of the calculated global minimum structures to experimental ones.[8] We see, that the trends for the hydrogen bonds are reproduced in both cases, the dimer **I** and the trimer **IV**. The hydrogen bond for the dimer structure is predicted to be 5 pm shorter than the experimental value with both functionals, BLYP and B3LYP, respectively. The N−N−O angle is 13 and 19 deg larger in the calculations. For the trimer structure again the N−H bond is considerably shorter in the calculations (12 pm). The N−O distance is shorter by 7 pm in the theoretical calculations. The angles on the other hand are within a few degrees. The consistency between the two functionals, together with the large basis set used in the calculations, let us be rather confident in the calculated values. It also has to be considered that the derivation of the experimental structures depends on interpretation and a non trivial fitting procedure. However, it cannot be excluded that we encounter here a deficiency of the density functional theory. Only calculations with correlated wave function methods can settle this point.

In a recent paper, Adamo and Barone[21] investigated solvent shifts of transitions in s-tetrazine with the polarizable continuum model combined with cluster models. They used a cluster of four water molecules hydrogen bonded to the four nitrogen atoms of s-tetrazine. After a geometry optimization in D_{2h} symmetry, they report an interaction energy of 28.5 kJ/mol per water molecule. This calculation was performed at the PBE0/6-311++G(d,p) level including BSSE corrections. We performed several optimizations of different structures using our standard basis and the B3LYP functional. Within D_{2h} symmetry interaction energies of 7.8 and 9.8 kJ/mol for structures similar to the one in ref 21 and the same with rotated water molecules were found, respectively. The most stable structure of this type was achieved by relaxing the symmetry constraint and resulted in a binding energy of 15.5 kJ/mol per molecule. We also tested that the differences are not due to the different functionals. We

TABLE 6: Vertical Excitations of Low Lying States of Dimer I (Upper Part) and Trimer IV (Lower Part)[a]

character	main transition	BLYP	B3LYP
n → π*	HOMO → LUMO	1.91 (0.03)	2.24 (0.03)
n → π*	HOMO → LUMO + 1	2.92 (0.06)	3.45 (0.07)
n → π*	HOMO − 2 → LUMO	4.08 (−0.04)	4.74 (0.02)
π → π*	HOMO − 3 → LUMO	5.38 (0.01)	5.70 (−0.01)
n → π*	HOMO → LUMO	1.91 (0.03)	2.23 (0.02)
n → π*	HOMO → LUMO + 1	2.96 (0.10)	3.48 (0.10)
n → π*	HOMO − 2 → LUMO	4.12 (0.00)	4.78 (0.06)
π → π*	HOMO − 3 → LUMO	5.35 (−0.02)	5.67 (−0.04)

[a]Values are in eV. Differences from the corresponding excitation in s-tetrazine are given in parentheses.

therefore must conclude that the argument for the stability of such s-tetrazine water clusters in liquid solution given in ref 21 does not hold.

Table 6 lists the vertical excitation energies of dimer **I** and trimer **IV**. The first two transitions (the $1B_{3u}$ and the $1A_u$ in the isolated tetrazine) show a small hypsochromic shift, i.e., a blue shift with increasing solvent polarity, also called negative solvatochromism. A small red shift is found in both clusters for the first $\pi \rightarrow \pi^*$ transition. All the shifts are considerably smaller than experimental values and we can conclude that the contribution to the solvent shift by hydrogen bonding is minor. In addition to the transitions shown in Table 6 several charge transfer (CT) states appear in the calculated spectra. These states are characterized by transitions from the HOMOs of the water molecules to the LUMO of s-tetrazine. The transition energies are only slightly different from the orbital energy differences. Therefore, the CT states appear for the BLYP functional considerably lower in energy than for the hybrid B3LYP functional. In the dimer case we find the first CT state at 2.37 eV for BLYP and 4.35 eV for B3LYP. The appearance of these states makes it more difficult to find the first $\pi \rightarrow \pi^*$ transition. For example, this state is only at 11th position in the dimer spectra with the BLYP functional. This is a direct consequence of the well-known failure of standard density functionals to describe properly CT excitations[20,58,59] and as we will see has practical implications for the calculation of excitation spectra in solution (see section 5). This problem and its implications has recently been investigated for the case of the acetone molecule in water solution.[59]

5. Macrosolvation: Car−Parrinello Simulations

Radial distribution functions (RDFs) for the solute−solvent interactions were calculated for different atoms. The RDFs for the nitrogen and methenyl groups in s-tetrazine are presented in Figure 4. There is only a weak feature in the $N-H_{water}$ RDF at a distance of 2 Å, which corresponds to hydrogen bonds accepted by s-tetrazine. Surprisingly, a more pronounced feature is seen below 2.5 Å for water oxygen around methenyl hydrogens. We calculated the running number of hydrogen bonds being accepted and donated by the solute. From these curves in Figure 5, it is clear that the existing hydrogen bonds are weak and have a short lifetime. Moreover, the solute shows an almost equal propensity for donating as for accepting hydrogen bonds. The definition of a hydrogen bond (X−H--Y) was $r_{HY} < 2.6$ and $\delta_{XHY} > 150°$. Although the distance definition was not adapted to the CH−O hydrogen bond (the acceptable angles were changed to >120°), which is considerably longer than a typical OH−O hydrogen bond, we observe that the number of donated hydrogen bonds is even higher on average than the number of accepted hydrogen bonds. The picture of the hydration of s-tetrazine, which is obtained from the CPMD simulation is

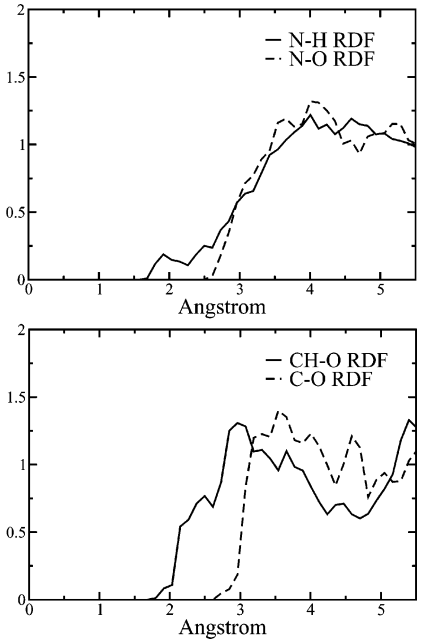

Figure 4. Radial distribution functions (RDFs) for hydrogen accepting and donation groups in s-tetrazine. The peaks around 2 Å in the $N-H_{water}$ (top) and 2.3 Å in the $H_{s-tetrazine}-O$ (bottom) RDFs show that hydrogen bonding occurs.

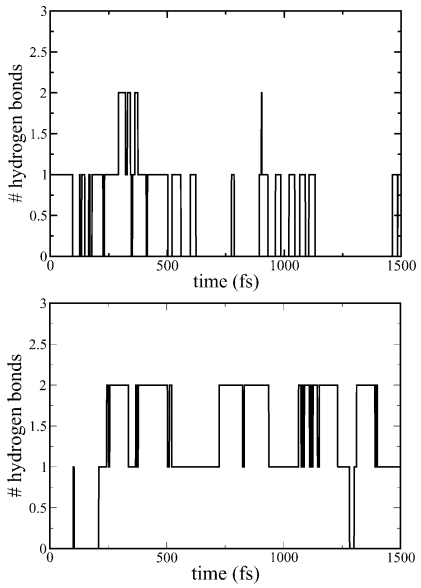

Figure 5. Fluctuations in the number of hydrogen bonds (accepted and donated by s-tetrazine) during the MD trajectory. The top panel shows hydrogen bonds to the nitrogen atoms and the bottom panel hydrogen bonds involving the CH group.

therefore consistent with the conclusions drawn from the cluster calculations. There is a clathrate-like structure formed around the solute and no stable hydrogen-bonded complex with water is observed. As mentioned before, this behavior can be rationalized from the interaction energies calculated for the s-tetrazine−water clusters. The strongest hydrogen bond with an interaction energy similar to the water dimer is achieved with a double contact structure (see Figure 3 structure **I**). However, such a structure would eliminate two hydrogen bonds within the water network and is therefore unlikely. In fact, during the CPMD simulation, no such structure could be found. The single contact structures are considerably weaker and therefore also not favored. The fact that the s-tetrazine is situated in a solvent cage within the water hydrogen bond network changes this situation

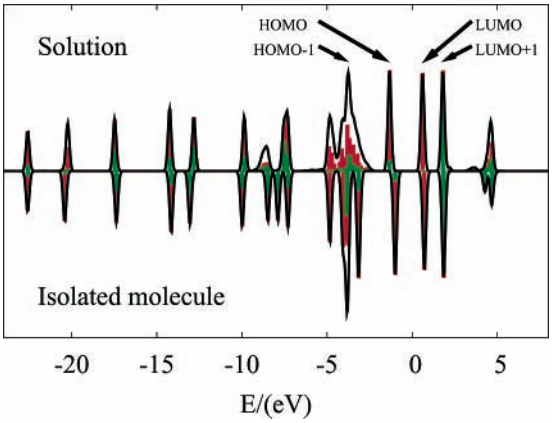

Figure 6. Local density of states (LDOS) on s-tetrazine in aqueous solution (positive intensity) and the single molecule (negative intensity). The discrete spectrum (green bars) is presented together with the partial carbon character (red bars). A convolution of the discrete spectrum with a Gaussian of fixed width is also shown. The energy of the lowest (most inert) solute valence orbital (at ≈ -22 eV) was used to align the spectra. The HOMO−LUMO gap is used to define an origin on the energy scale. The LDOS from aqueous solutions is calculated for an arbitrary snapshot along the molecular dynamics trajectory. The single molecule LDOS is calculated at the optimized structure.

considerably. First-shell water molecules face a surface where no other water molecules offer the possibility of hydrogen bonding and rather than having no hydrogen bond a hydrogen bond to s-tetrazineis preferred. As the interaction energies for donating and accepting hydrogen bonds are comparable both scenarios are recorded. The four accepting groups are slightly less active than the two donating groups. This is most likely due to the more exposed nature of the s-tetrazine hydrogens, their higher flexibility, and the slightly higher interaction energies.

Before presenting the calculations of the excited states, we discuss the density of states of the occupied orbitals. For this purpose the local density of states on the solute (LDOS) was computed by projection of each orbital on a minimal Slater type basis at each atom, and summing up the square of the coefficients on the carbon and nitrogen atoms. In Figure 6, the LDOS spectrum of s-tetrazine in aqueous solution is compared to that of the single molecule.

First of all, we notice that this comparison agrees well with the general picture of the observed solvent shifts in the optical spectrum. The HOMO and to less an extent the LUMO are polarized and shifted downward in energy by the solvent, whereas the LUMO+1 is not effected. The difference in polarization of the HOMO and LUMO+1 gives rise to the large blue shift in the A_u excitation (HOMO $\rightarrow$ LUMO+1) in aqueous solution. Since the LUMO also experience some polarization, the B_{3u} excitation (HOMO $\rightarrow$ LUMO) only shows a minor blue shift in aqueous solution, and the B_{2u} excitation (HOMO-3 $\rightarrow$ LUMO) shows a minor red shift since the HOMO-3 is not affected by the solvent.

Second, we notice that the peaks in the interval [−9, −8 eV] in the gas phase spectrum are shifted and have lost intensity in the aqueous solution due to mixing with solvent orbitals. This mixing is not necessarily a signature of strong interactions (e.g., hydrogen bonding) but is simply an effect of a high density of states of the solvent in this region. The distribution of the solute orbitals over a large number of states has practical implication for the calculation of the optical spectrum discussed later.

We also studied the time evolution of the Kohn−Sham energies, showing large fluctuations (±0.5 eV) in the energies around the band gap. An exception to this behavior is the energy of LUMO+2. This state is a mixture of a Rydberg-like state of the solute and the conduction band of the solvent. The energy of this state is almost constant (±0.05 eV) over the whole simulation.

The electronic spectrum was calculated at regular intervals during the molecular dynamics simulation, which enables us to perform dynamical averaging and to identify which molecular interactions are causing the solvent shifts.

There are several technical problems encountered in calculating the optical spectrum for the solute in an aqueous solution within a density functional framework. Because of the large number of electronic states and since each excited state requires a separate linear response wave function, the number of excited states that can be calculated is strongly limited by the memory of the computer. Hence, only the first four excited states could be calculated employing the Tamm−Dancoff approximation, and of these three were typically charge-transfer (CT) transitions from the solvent to the solute orbitals. However, these CT excitation are too low in energy due to deficiencies in the approximative functional (BLYP) and the adiabatic approximation to TDDFT.[58,59] The problem is only partially solved by the inclusion of exact exchange in the B3LYP calculations, in which the corresponding excitations are and still below the A_u excitation for example. Even if the CT were correctly described the large number of them would make it impossible to reach higher excited states of the solute, like the $\pi \rightarrow \pi^*$ transition, in a system like the one we studied.

The memory "bottleneck" can be resolved by limiting the number of occupied orbitals involved in the transitions, which determines the memory requirements of the linear response wave functions. This approximation is only applicable to excitations that involve orbitals which are not strongly mixed with those of the solvent and could be used in our case to obtain the lowest two $n \rightarrow \pi^*$ singlet excitations. These involve only the HOMO, LUMO, and LUMO+1, which essentially remain localized on the solute as seen in Figure 6. In principle, the subspace approach could also be used to calculate the $\pi \rightarrow \pi^*$ excitation since it seems to lie below the region of high DOS from the solvent. However, we did not make the effort to find the orbital to include for each snapshot in the simulation trajectory. The region which mixes strongly with the low-lying nitrogen lone-pair orbitals contains in our simulation between 50 and 100 orbitals. To include all low-lying excitations from the nitrogen lone-pairs, we employ the method of localization of the occupied orbitals in a periodic system.[55,56] After the localization, we can for s-tetrazine limit the subspace method to the 15 Wannier orbitals arising from the solute. It is easily determined which are the solute orbitals from the distance of the orbitals charge center and a solute atom.

The results from the localized subspace Tamm−Dancoff approximation [LOC−SUBTDA], averaged over the snapshots from the molecular dynamics simulation, is presented in Table 7. Even within the LOC−SUBTDA framework, there are CT excitations present. The solute-to-solvent CT excitations are not excluded in LOC−SUBTDA, since only the occupied orbitals are localized and selected in the subspace. For s-tetrazine(aq) it was still possible to find all the molecular excitations of interest among the first 20 excitations. The excitation energies, in particular the A_u transition, show large fluctuations which are due to a strong dependence of the transitions on the solvent structure and can be directly related to the fluctuations in the Kohn−Sham energies.

Complementary TDDFT calculations of the isolated s-tetrazine molecule and clusters with one water molecule show

TABLE 7: Solvent Shifts in the Vertical Excitation Energies (within the Tamm−Dancoff Approximation) of Singlet Excitations in s-Tetrazine (eV)[a]

model method	expt[b]	CPMD BLYP	CPMD/MM BLYP[c]
B_{3u}, n → π^*	+0.18	0.17 ± 0.03	0.17 ± 0.03
A_u, n → π^*	+0.18[d]	0.27 ± 0.10	0.15 ± 0.11
B_{1g}, n → π^*		0.16 ± 0.02	0.13 ± 0.02
B_{2u}, π → π^*	−0.08	−0.06 ± 0.02	−0.09 ± 0.02

[a] The CPMD results are calculated from 12 snapshots and the error uncertainty in the A_u is largely due to large fluctuations in this state. [b] From ref 1. [c] The QM/MM results are calculated at the geometries obtained with the full quantum MD simulation. [d] Shift from transition in cyclohexane.

that the solvent shift in the A_u excitation is not due to the instantaneous nonplanar geometries of s-tetrazine in aqueous solution or to [CH−O] hydrogen bonding. The solvent shift in the A_u excitation is due to polarization. This is supported by comparison to the QM/MM solvent shifts (see Table 7), which for each time frame are within 0.1 eV of the full CPMD results despite the large fluctuations (±0.5 eV) in the excitation energy. Furthermore, QM/MM calculations with the B3LYP functional on one of the MD snapshots showed that the inclusion of exact exchange does not change the A_u solvent shift. These findings are consistent with studies on the solvent effects on nitrogen NMR shieldings.[57]

6. Summary and Conclusions

Density functional based calculations of s-tetrazine, its adducts with water, and an aqueous solution of s-tetrazine have been carried out. Using the BLYP and B3LYP functionals results from earlier density functional calculations with pure density and hybrid functionals[20,21] for the ground and excited states of s-tetrazine are reproduced. The results for optimized geometries and harmonic frequencies are in good agreement with wave function based correlation calculations. Excitation energies for the first three n → π^* states agree also with these calculations, however without reaching full quantitative agreement. In accordance with EOM-CC[15] calculations both density functionals employed predict the ^1A_u state in D_{2h} symmetry to be a first-order saddle point. The overall performance of the DFT calculations in these test calculations show that reliable simulations of s-tetrazine in its ground and excited states can be performed using the BLYP functional.

The most stable s-tetrazine/water complex was calculated to display a homodromic feature: One water hydrogen builds a slightly bend hydrogen bond to the nitrogen lone pair, whereas the other water's oxygen lone pair is in interaction distance to the hydrogen atom of s-tetrazine. The interaction energy of this complex (17.7 kJ/mol for B3LYP) is found to be almost twice as large as the value for a double O−H···N arrangement (11.1 kJ/mol) or for a linear C−H···O geometry (10.0 kJ/mol). Stable complexes with π bonding are considerably weaker. These results already point to the importance of the weak hydrogen bond structure for the solvation of s-tetrazine in water. It is the structure with the almost linear C−H···O geometry that provides the highest bonding energy per occupied water hydrogen donor/acceptor site. This is confirmed in the Car−Parrinello molecular dynamics simulation where the radial distribution functions clearly show a preference of water for hydrogen bonding to the C−H group over the nitrogen lone pairs. Using geometrical definitions for hydrogen bonding the same effect can also be shown in plotting the number and types of hydrogen bonds along the simulation trajectory. From these simulations emerges a picture for the solvation of s-tetrazine in water where the solute molecule is placed in a water cave with weak bonding to its hydrogen atoms and occasional short-lived hydrogen bonds to the nitrogen atoms. Another indication of the solvation structure was gained from the optimized structures of s-tetrazine with two water molecules. The second water molecule prefers a position where it establishes a hydrogen bond to the other water molecule and has an almost optimal position for the weak hydrogen bonding to the s-tetrazine hydrogen atom. The interaction energy of this three hydrogen bond ring structure shows a strong cooperative effect.

Comparison of the geometries of the s-tetrazine/water complexes with structures derived from experiment[8] show generally good agreement. However, the nitrogen water hydrogen bond is calculated for both clusters to be about 6 and 12 pm shorter. The values found for the two functionals, BLYP and B3LYP, are consistent. Highly correlated wave function calculations will be necessary to decide if the density functionals fail to accurately predict the bonding situation or if the experimental raw data needs reinterpretation.

Calculations of vertical excitations using the Tamm−Dancoff approximation to TDDFT showed that the solvent shifts can be explained from the polarization of the Kohn−Sham orbitals of the solute. HOMO and to a lesser extend LUMO are shifted downward in energy, whereas LUMO+1 is not affected by the solvent. This results in blue shifts for the first excited state (HOMO → LUMO) and the A_u (HOMO → LUMO+1) state. The HOMO-3 state is not affected by the solvent and therefore the first π → π^* state (HOMO-3 → LUMO) shows a red shift. Excitation energies are remarkably stable along the trajectory except for the A_u state were fluctuation of 0.2 eV are found. The interpretation of the origins of solvent shifts was confirmed by QM/MM[42] calculations where only the solute molecule was treated quantum mechanically. The TDDFT calculations of the solute/solvent system suffered from the problem of too small band gaps of current density functionals (BLYP in our case). To avoid the calculation of hundreds of spurious charge transfer states between solvent molecules, the active space for excitation had to be limited to the subspace spawned by the localized orbitals of the solute molecule.

Acknowledgment. This work was supported in part by the Swiss National Science Foundation (No. 21-63305.00 and No. 200020-100417) and a Forschungskredit of the University of Zurich.

Supporting Information Available: Tables of highest occupied and lowest unoccupied Kohn−Sham orbitals of s-tetrazine, geometries of s-tetrazine in the ground state as obtained with different methods, and harmonic frequencies of s-tetrazine in the ground state as obtained with different methods. This material is available free of charge via the Internet at http://pubs.acs.org.

References and Notes

(1) Innes, K. K.; Ross, I. G.; Moomaw, W. R. *J. Mol. Spectrosc.* **1988**, *132*, 492.
(2) Palmer, M. H.; McNab, H.; Reed, D.; Walker, A. P. I. C.; Guest, M. F.; Siggel, M. R. F. *Chem. Phys.* **1997**, *214*, 191.
(3) Smalley, R. E.; Wharton, L.; Levi, D. H.; Chandler, D. W. *J. Mol. Spectrosc.* **1977**, *66*, 375.
(4) Young, L.; Haynam, C. A.; Levi, D. H. *J. Chem. Phys.* **1983**, *79*, 1592.
(5) Haynam, C. A.; Brumbaugh, D. V.; Levi, D. H. *J. Chem. Phys.* **1983**, *80*, 2256.
(6) Haynam, C. A.; Brumbaugh, D. V.; Levi, D. H. *J. Chem. Phys.* **1983**, *79*, 1581.

(7) Haynam, C. A.; Morter, C.; Young, L.; Levi, D. H. *J. Phys. Chem.* **1987**, *91*, 2519.
(8) Haynam, C. A.; Morter, C.; Young, L.; Levi, D. H. *J. Phys. Chem.* **1987**, *91*, 2526.
(9) Mason, S. F. *J. Chem. Soc.* **1959**, 1240.
(10) Scheiner, A. C.; Schaefer, H. F. *J. Chem. Phys.* **1987**, *87*, 3539.
(11) Ghosh, S.; Chowdhury, M. *Chem. Phys. Lett.* **1982**, *85*, 233.
(12) Innes, K. K. *J. Mol. Spectrosc.* **1988**, *129*, 140.
(13) Ågren, H.; Knuts, S.; Mikkelsen, K. V.; Jensen, H. J. A. *Chem. Phys.* **1992**, *159*, 211.
(14) Schütz, M.; Hutter, J.; Lüthi, H. P. *J. Chem. Phys.* **1995**, *103*, 7048.
(15) Stanton, J. F.; Gauss, J. *J. Chem. Phys.* **1996**, *104*, 9859.
(16) Del Bene, J. E.; Watts, J. D.; Bartlett, R. J. *J. Chem. Phys.* **1997**, *106*, 6051.
(17) Rubio, M.; Roos, B. O. *Mol. Phys.* **1999**, *96*, 603.
(18) Nooijen, M. *Spectrochim. Acta, Part A* **1999**, *55*, 539.
(19) Hamprecht, F. A.; Cohen, A. J.; Tozer, D. J.; Handy, N. C. *J. Chem. Phys.* **1998**, *109*, 6264.
(20) Tozer, D. J.; Amos, R. D.; Handy, N. C.; Roos, B. O.; Serrano-Andrés, L. *Mol. Phys.* **1999**, *97*, 859.
(21) Adamo, C.; Barone, V. *Chem. Phys. Lett.* **2000**, *330*, 152.
(22) Tomasi, J.; Persico, M. *Chem. Rev.* **1994**, *94*, 2027.
(23) Perdew, J. P.; Burke, K.; Ernzerhof, M. *Phys. Rev. Lett.* **1996**, *77*, 3865.
(24) Adamo, C.; Barone, V. *J. Chem. Phys.* **1999**, *110*, 6158.
(25) Car, R.; Parrinello, M. *Phys. Rev. Lett.* **1985**, *55*, 2471.
(26) Ahlrichs, R.; Bär, M.; Häser, M.; Horn, H.; Kölmel, C. *Chem. Phys. Lett.* **1989**, *162*, 165.
(27) Dunning, T. H. *J. Chem. Phys.* **1989**, *90*, 1007.
(28) Kendall, R. A.; Dunning, T. H.; Harrison, R. J. *J. Chem. Phys.* **1992**, *96*, 6796.
(29) The turbomole basis set library is available via anonymous ftp from ftp://ftp.chemie.uni-karlsruhe.de/pub/basen.
(30) Furche, F.; Ahlrichs, R. *J. Chem. Phys.* **2002**, *117*, 7433.
(31) Neugebauer, J.; Reiher, M.; Kind, C.; Hess, B. A. *J. Comput. Chem.* **2002**, *23*, 895.
(32) Boys, S. F.; Bernardi, F. *Mol. Phys.* **1970**, *19*, 553.
(33) CPMD V3.7 Copyright IBM Corp 1990−2003, Copyright MPI für Festkörperforschung Stuttgart 1997−2001.
(34) Marx, D.; Hutter, J. In *Modern Methods and Algorithms of Quantum Chemistry*; NIC Series 1; Grotendorst, J., Ed.; FZ Jülich: Jülich, Germany, 2000; pp 329−477.
(35) Kleinman, L.; Bylander, D. M. *Phys. Rev. Lett.* **1982**, *48*, 1425.
(36) Giannozzi. P. 1993, Potential of the form $-Z/r\ \mathrm{erf}[r/r_c] + (a + br^2)\exp[-(r/r_{cl})^2]$ with the following parameters for hydrogen: $Z = 1$, $r_c = 0.25$, $r_{cl} = 0.2829559$, $a = -1.9615990$, and $b = 0.405181$.
(37) Troullier, N.; Martins, J. L. *Phys. Rev. B* **1991**, *43*, 1993.
(38) Nosé, S. *J. Chem. Phys.* **1984**, *81*, 511.
(39) Hoover, W. G. *Phys. Rev. A* **1985**, *31*, 1695.
(40) Jorgensen, W. L.; Chandrasekhar, J.; Madura, J. D.; Impey, R. W.; Klein, M. L. *J. Chem. Phys.* **1983**, *79*, 926.
(41) Cornell, W. D.; Cieplak, P.; Bayly, C. I.; Gould, I. R.; Merz, K. M.; Ferguson, D. M.; Spellmeyer, D. C.; Fox, T.; Caldwell, J. W.; Kollman, P. A. *J. Am. Chem. Soc.* **1995**, *117*, 5179.
(42) Laio, A.; VandeVondele, J.; Rothlisberger, U. *J. Chem. Phys.* **2002**, *116*, 6941.
(43) Hirata, S.; Head-Gordon, M. *Chem. Phys. Lett.* **1999**, *314*, 291.
(44) Hutter, J. *J. Chem. Phys.* **2003**, *118*, 3928.
(45) Becke, A. D. *Phys. Rev. A* **1988**, *38*, 3098.
(46) Lee, C.; Yang, W.; Parr, R. G. *Phys. Rev. B* **1988**, *37*, 785.
(47) Becke, A. D. *J. Chem. Phys.* **1993**, *98*, 5648.
(48) Stephens, P. J.; Devlin, F. J.; Chabalowski, C. F.; Frisch, M. J. *J. Chem. Phys.* **1994**, *98*, 11623.
(49) Nooijen, M. *J. Phys. Chem. A* **2000**, *104*, 4553.
(50) Rauhut, G.; Werner, H. J. *Phys. Chem. Chem. Phys.* **2003**, *5*, 2001.
(51) Parac, M.; Grimme, S. *J. Phys. Chem. A* **2002**, *106*, 6844.
(52) Desiraju, G. R.; Steiner, T. The Weak Hydrogen Bond. *Structural Chemistry and Biology*; Oxford University Press: Oxford, England, 1999.
(53) Li, X.; Liu, L.; Schlegel, H. B. *J. Am. Chem. Soc.* **2002**, *124*, 9639.
(54) Kirchner, B.; Reiher, M. *J. Am. Chem. Soc.* **2002**, *124*, 6206.
(55) Marzari, N.; Vanderbilt, D. *Phys. Rev. B* **1997**, *56*, 12847.
(56) Berghold, G.; Mundy, C. J.; Romero, A. H.; Hutter, J.; Parrinello, M. *Phys. Rev. B* **2000**, *61*, 10040.
(57) Witanowski, M.; Biedrzycka, Z.; Sicinska, W.; Grabowski, Z.; Webb, G. A. *J. Magn. Reson.* **1997**, *124*, 127.
(58) Dreuw, A.; Weisman, J. L.; Head-Gordon, M. *J. Chem. Phys.* **2003**, *119*, 2943.
(59) Bernasconi, L.; Sprik, M.; Hutter, J. *J. Chem. Phys.* **2003**, *119*, 12417.